Molecules and Cells

# Tsg101 Is Necessary for the Establishment and Maintenance of Mouse Retinal Pigment Epithelial Cell Polarity

Dai Le[1,3], Soyeon Lim[1,3], Kwang Wook Min[1], Joon Woo Park[1], Youjoung Kim[1], Taejeong Ha[1], Kyeong Hwan Moon[1], Kay-Uwe Wagner[2], and Jin Woo Kim[1,*]

[1]Department of Biological Sciences, Korea Advanced Institute of Science and Technology (KAIST), Daejeon 34141, Korea, [2]Department of Oncology, Wayne State University, Detroit, MI 48201, USA, [3]These authors contributed equally to this work.
*Correspondence: jinwookim@kaist.ac.kr
https://doi.org/10.14348/molcells.2021.0027
www.molcells.org

**The retinal pigment epithelium (RPE) forms a monolayer sheet separating the retina and choroid in vertebrate eyes. The polarized nature of RPE is maintained by distributing membrane proteins differentially along apico-basal axis. We found the distributions of these proteins differ in embryonic, post-natal, and mature mouse RPE, suggesting developmental regulation of protein trafficking. Thus, we deleted *tumor susceptibility gene 101* (*Tsg101*), a key component of endosomal sorting complexes required for transport (ESCRT), in embryonic and mature RPE to determine whether ESCRT-mediated endocytic protein trafficking correlated with the establishment and maintenance of RPE polarity. Loss of *Tsg101* severely disturbed the polarity of RPE, which forms irregular aggregates exhibiting non-polarized distribution of cell adhesion proteins and activation of epidermal growth factor receptor signaling. These findings suggest that ESCRT-mediated protein trafficking is essential for the development and maintenance of RPE cell polarity.**

**Keywords:** cell polarity, endosomal sorting complexes required for transport (ESCRT), retinal pigment epithelium (RPE), *tumor susceptibility gene 101* (*Tsg101*)

## INTRODUCTION

In vertebrate eyes, the retinal pigment epithelium (RPE) interacts with the outer segments of photoreceptors on its apical side and with the extracellular matrix of Bruch's membrane on its basal side (Lehmann et al., 2014; Weisz and Rodriguez-Boulan, 2009). The RPE supports the survival and functions of photoreceptors by absorbing light scattered from the outer segments of photoreceptors; by participating in the visual cycle of photopigments; by capturing toxic metabolic wastes from photoreceptors; by providing nutrients from choroidal capillaries to the retina via trans-epithelial transport; and by engulfing the outer segments of photoreceptors and dead photoreceptors (Simó et al., 2010; Strauss, 2005).

Structural and functional defects in the RPE frequently result in dysfunction and/or degeneration of the photoreceptors, causing various retinal degenerative diseases, including retinitis pigmentosa, retinal detachment, and age-related macular degeneration (Kang et al., 2009; Marmorstein, 2001; Veleri et al., 2015). Its unique functions in vision therefore require the RPE to maintain a polarized distribution of many proteins (Bonilha et al., 1999; Finnemann et al., 1997; Fujimura et al., 2009; Shimura et al., 1999). To date, however, the underlying molecular mechanisms responsible for the establishment and maintenance of a polarized protein distri-

Received 2 February, 2021; revised 2 March, 2021; accepted 2 March, 2021; published online 28 March, 2021

eISSN: 0219-1032

bution in the RPE remain incompletely understood.

Following their synthesis in the endoplasmic reticulum, membrane proteins in epithelial cells are delivered to various intracellular membranous compartments by exocytic vesicles derived from the Golgi apparatus (Rodriguez-Boulan and Macara, 2014). Later, the proteins, however, can be redistributed to other membranous compartments from initial sites by endocytic transport (Le Borgne and Hoflack, 1998; Mellman and Nelson, 2008; Rodriguez-Boulan and Macara, 2014; Shivas et al., 2010; Williams et al., 1984). Therefore, the polarized distribution of membrane proteins in epithelial cells can result from both exocytosis and endocytosis.

Proteins in the plasma membrane are loaded onto endosomes and subsequently transferred to lysosomes by endosome-lysosome fusion, resulting in the degradation or re-routing of these proteins to other cellular membrane compartments. During the course of endo-lysosomal maturation, many membrane proteins in endosomes can be sorted further into multivesicular bodies (MVBs). The intra-MVB vesicular trafficking removes endosomal membrane proteins from cytoplasm, where their functional sites are exposed. Consequently, cytoplasmic events mediated by membrane receptors, such as epidermal growth factor receptor (EGFR), are terminated by MVB trafficking (Eden et al., 2009). Proteins in the intra-MVB vesicles, also called exosomes, are often released into extracellular space following fusion of the MVBs with the plasma membrane (Grant and Donaldson, 2009; Gruenberg and Stenmark, 2004; Hurley, 2010; Schmidt and Teis, 2012). Fusion of these MVB-derived extracellular vesicles with the plasma membrane can lead to the reintegration of these membrane proteins into the plasma membrane (Clague et al., 2012), resulting in the transfer of the proteins autonomously and non-autonomously.

Therefore, the endosomal sorting complexes required for transport (ESCRT), which is responsible for the formation of MVB (Babst, 2011; Gruenberg and Stenmark, 2004), starts to receive a focus as an intercellular communication machinery in addition to its classical role in the endo-lysosomal proteins degradation. The ESCRTs have been subdivided into four major complexes: ESCRT-0, -I, -II, and -III. The components of ESCRT-0, including hepatocyte receptor tyrosine kinase substrate (Hrs)/vacuolar protein sorting 27 (Vps27) and signal transducing adapter molecule 1 (Stam1), capture ubiquitinated proteins, transferring them to ESCRT-I and subsequently to ESCRT-II and -III for intra-endosomal vesicular sorting to form MVBs (Hurley, 2010; Schmidt and Teis, 2012). Membrane proteins in the endosomes are also subjected to ESCRT-mediated intra-endosomal vesicular trafficking, although ESCRT-0 is not essential for MVB formation.

The present study examined the roles of ESCRT-mediated protein trafficking in mouse RPE by eliminating *tumor susceptibility gene 101* (*Tsg101*), which encodes an ESCRT-I component Tsg101, also called vascular protein sorting 23 (Vps23). Deletion of *Tsg101* abrogated the polarity in mouse RPE, which form an irregular multilayer structure. In the *Tsg101*-deficient mouse RPE, the phosphoinositide 3-kinase (PI3K)-Akt and mitogen-activated protein kinase (MAPK) pathways, which can disrupt RPE polarity (Kang et al., 2009; Kim et al., 2008), were also found to be activated at downstream of EGFR, which is subjected to the ESCRT-mediated downregulation (Eden et al., 2009). These results suggest that the ESCRT-mediated protein trafficking is necessary for the establishment and maintenance of RPE cell polarity.

## MATERIALS AND METHODS

### Mouse lines

*Tag101*$^{fl/fl}$ mice were generated as described previously, and used to breed with various Cre lines and *R26R* mice to generate the mice used in this study (Iacovelli et al., 2011; Mori et al., 2002; 2012; Rowan and Cepko, 2004; Soriano, 1999; Wagner et al., 2003). Mice were genotyped according to the published protocols. Samples were collected and analyzed between littermates. All mice used in this study were maintained in a specific pathogen-free facility of Korea Advanced Institute of Science and Technology (KAIST) Laboratory Animal Resource Center. All experiments were performed according to the Korean Ministry of Food and Drug Safety (MFDS) guidelines for animal research. The protocols were certified by the Institutional Animal Care and Use Committee (IACUC) of KAIST (KA-2014-20).

### Immunohistochemistry

Immunohistochemistry of cryosection was done as described in previous report (Kim et al., 2008). Briefly, mice are perfused and then adult eyes samples are fixed overnight in 4% paraformaldehyde at 4°C, whereas embryonic heads are fixed for 4 h at 4°C. Heat-induced antigen retrieval was also performed with citrate buffer (10 mM sodium citrate, 0.05% Tween-20, pH 6.0) when necessary. Samples were incubated in blocking solutions (phosphate-buffered saline [PBS] with 0.5% Triton X-100 + 5% normal serum for embryonic eyes and PBS with 1% Triton X-100 + 10% normal serum for adult eyes). Samples are incubated with primary antibodies diluted in blocking solution (1:100 v/v) overnight at 4°C. Secondary antibodies are diluted in blocking solution (1:200 v/v) for 1 h at room temperature. Hoechst staining is done for 15 min at room temperature following secondary antibodies incubation. Antibodies used in this study are provided in Supplementary Table S1.

The immunostaining images were then acquired using Olympus FV1000 confocal microscope and manipulated by the Photoshop CS6 and Bitplane Imaris 6.3.1 softwares.

### Electron microscopy

Transmission electron microscopy (TEM) analyses were done as described previously (Ha et al., 2017; Kim et al., 2008). The eyes of were isolated from adult C56BL/6J mice perfused with a solution containing 2.5% glutaraldehyde and 2% paraformaldehyde in 0.1 M sodium cacodylate buffer (pH 7.2) in the morning and further fixed in the same solution for 24 h. Alternatively, embryonic mouse heads were isolated from the uterus and fixed for 24 h. The eyes and embryonic heads were then post-fixed with 1% OsO4 for 2 h on ice. The samples were stained and blocked with 0.5% uranyl acetate for 2 h, and then embedded in Epon 812 after dehydration. Ultrathin sections (80 nm) of the samples were then made and examined using an H-7000-type electron micro-

scope (Hitachi, Japan) operated at 75 kV.

### Electroretinogram (ERG) and OptoMotry

ERG measurements were done as described previously (Kim et al., 2017). In brief, mice were either dark- or light-adapted for 12 h and anesthetized with 2,2,2-tribromoethanol (Sigma, USA) in prior to dilating the pupils of the mice by 0.5% tropicamide. The mice were placed with a gold-plated objective lens on their corneas and silver-embedded needle electrodes at their foreheads and tails. The ERG recordings were performed using Micron IV retinal imaging microscope (Phoenix Research Labs, USA) and analyzed by Labscribe ERG software according to the manufacturer's instruction.

Mouse visual acuity was measured with the OptoMotry system (Cerebral Mechanics, USA) as previously described (Prusky et al., 2004). Mice adapted to ambient light for 30 min were placed on the stimulus platform surrounded by four computer monitors displaying black and white vertical stripe patterns. An event that mice track the stripe movements with reflexive head-turn was counted as a successful visual detection. The detection thresholds were then obtained from the OptoMotry software.

### Statistical analysis

All statistical analyses and graphs construction were done using IBM SPSS Statistics (ver. 20; IBM, USA). All data from statistical analysis are presented as the mean ± SD. Comparison between two groups was done by unpaired Student's *t*-test, and the differences among multiple groups were determined by ANOVA with Tukey's post-test. *P* values < 0.01 were considered as statistically significant results.

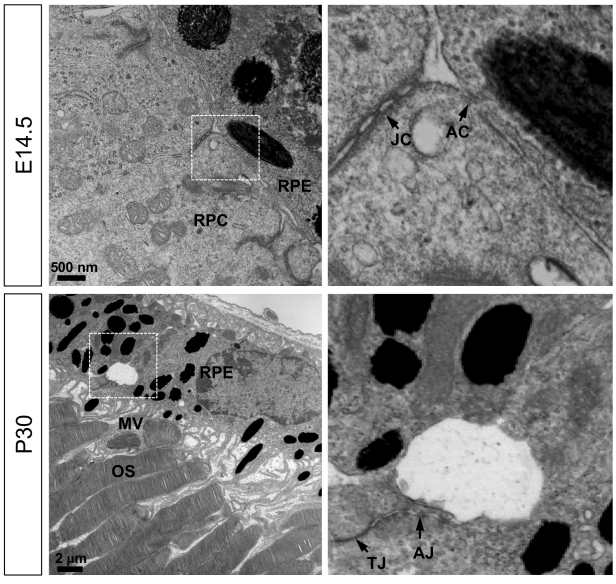


**Fig. 1. Structures of embryonic and adult mouse RPE.** TEM images of RPE-retina interphase of embryonic (E14.5) and adult (P30) mice (see details in the Materials and Methods section). Images in the right column are the magnified versions of the boxed areas in the left column. JC, junctional complex; AC, apical contact; MV, microvilli; OS, photoreceptor outer segment; TJ, tight junction; AJ, adherens junction.

## RESULTS

### Dynamic changes on the distribution of RPE polarity markers during development

Unlike the fully polarized characteristics of mature RPE, less is known about the polarity of embryonic RPE, which does not have recognizable microvilli on its apical side but forms focal contacts with adjacent retinal progenitor cell (RPC) (Fig. 1). The finding suggests that the expression and subcellular distribution of proteins responsible for interaction with adjacent retinal cells may differ in embryonic and mature RPE. Therefore, the distribution of various cell adhesion and polarity markers were assessed in mouse RPE from embryo to adult (Fig. 2, Supplementary Fig. S1, Table 1).

#### *P/E-cadherin*

Previously, placental and epithelial (P/E) cadherin protein and mRNA were shown to be expressed in adult RPE of adult mouse eyes and in culture (Burke and Hong, 2006; Burke et al., 1999), whereas only P-cadherin mRNA was identified in RPE of embryonic mouse eyes (Xu et al., 2002). We found that P/E-cadherin was expressed evenly in the RPE from embryonic day 12.5 (E12.5) to post-natal day 0 (P0) and then to be enriched at apical and basal sides of RPE at P7, when photoreceptors start to develop their outer segments (Figs. 2A-2D, Table 1). In mature RPE (i.e., P14 and P30), P/E-cadherin was found to be expressed strongly in the baso-lateral membrane but was not expressed in the apical membrane, as reported previously (Burke and Hong, 2006; Burke et al., 1999) (Figs. 2E and 2F, Table 1).

#### *N-cadherin*

N-cadherin was reported to be expressed in the baso-lateral membrane of mature RPE (Cachafeiro et al., 2013; Imamura et al., 2006), but on both sides in RPE of E10.5 mice (Fujimura et al., 2009). We also found that N-cadherin was detectable throughout the membrane areas of RPE in mice at E12.5 and E14.5 (Figs. 2G and 2H, Table 1). During the first post-natal week, N-cadherin expression was significantly reduced on the baso-lateral side but its expression was maintained strongly on the apical side (Figs. 2I and 2J, Table 1). From P14 onward, the level of N-cadherin expression was significantly reduced in RPE and was expressed only in the basal membrane at a low level (Figs. 2K and 2L, Table 1).

#### *β-catenin*

In agreement with previous findings on the expression of β-catenin in embryonic and mature RPE (Cachafeiro et al., 2013; Fujimura et al., 2009; Imamura et al., 2006), we found that β-catenin was highly expressed in RPE junctional areas at all stages (Figs. 2M-2R, Table 1). However, unlike its exclusive distribution in the adherens junctions (AJs) at the baso-lateral sides of mature RPE, β-catenin expression was not polarized in embryonic mouse RPE (Figs. 2M and 2N, Table 1). The results suggest that β-catenin may be involved in the apical contacts between the RPE and RPC as well as the AJs

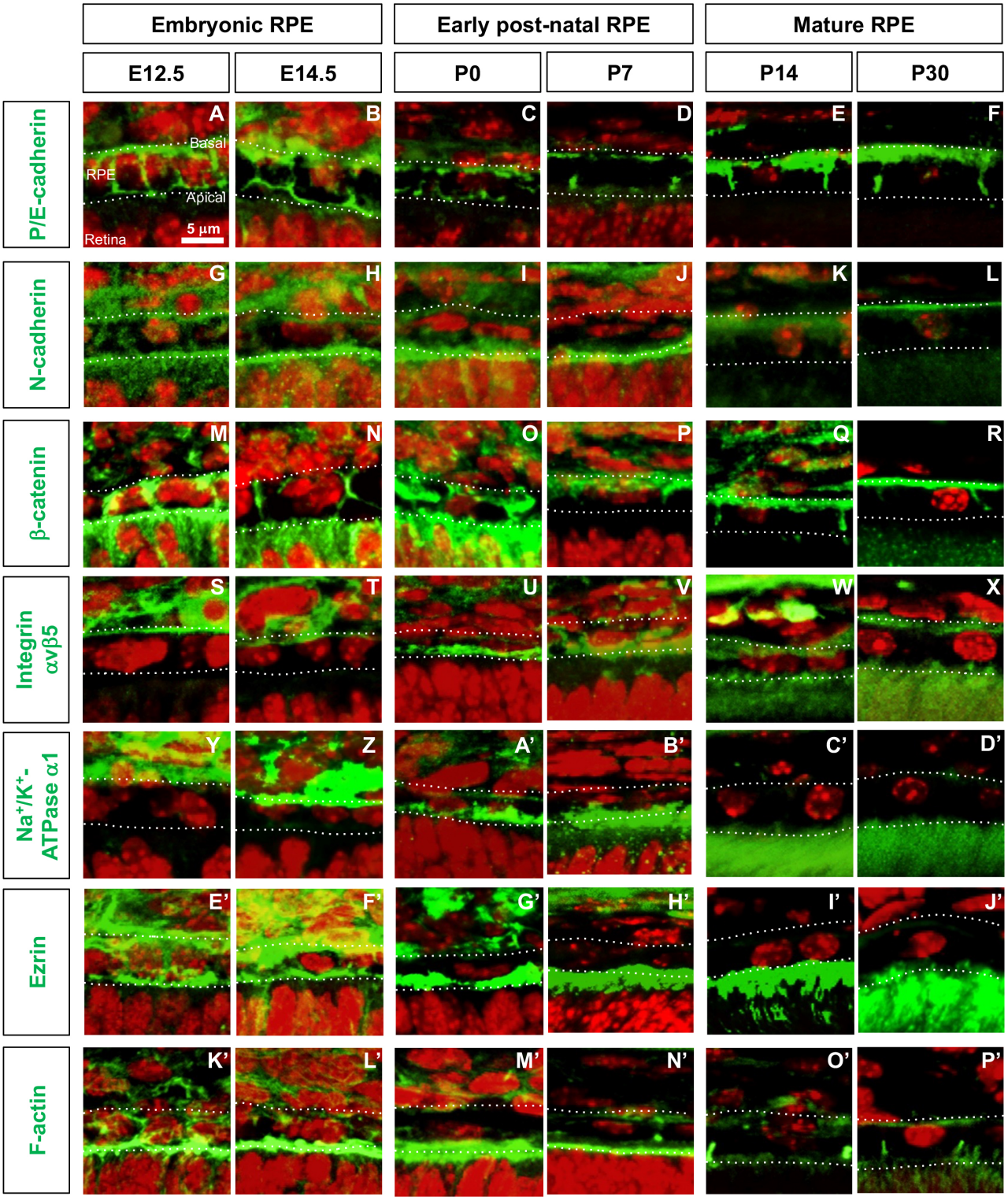


**Fig. 2. Distribution of cell polarity markers in developing mouse RPE.** (A-P') Distribution of corresponding proteins (green fluorescence signals) in embryonic (E12.5 and E14.5), post-natal (P0 and P7), and mature (P14 and P30) mouse RPE was investigated by immunostaining. Dash lines indicate basal and apical margins of RPE. Red fluorescence signals are the nuclei stained by Hoechst33342 (Hoe).

**Table 1**. Distribution of proteins in mouse RPE

| Protein name | Developmental stage | | | | | |
|---|---|---|---|---|---|---|
| | E12.5 | E14.5 | P0 | P7 | P14 | P30 |
| P/E-cadherin | NP | NP | NP | A, L | B, L | B, L |
| N-cadherin | NP | NP | A | A | B | B |
| β-catenin | NP | A, L | A, L | B, L | B, L | B, L |
| integrin αvβ5 | B | B | A | A | A, B | A, B |
| $Na^+/K^+$-ATPase α1 | B | B | A | A | A | A |
| Ezrin | NP | NP | A | A | A | A |

A, apical; B, basal; NL, non-polarized.

between the RPE in embryonic mouse eyes, later becoming concentrated at the inter-RPE AJs and basal membrane in mature mouse eyes.

### *Integrin αvβ5*

We found that integrin αvβ5 was expressed on both the apical and basal sides of mature mouse RPE (Figs. 2W and 2X, Table 1), as reported previously (Finnemann et al., 1997). During the embryonic period, however, integrin αvβ5 was expressed only on the basal side of RPE (Figs. 2S and 2T), whereas integrin αvβ5 expression in post-natal RPE was shifted to the apical membrane (Figs. 2U and 2V, Table 1).

### *$Na^+/K^+$-ATPase α1*

Similar to its expression in the apical membrane of cultured rat RPE (Gundersen et al., 1991), $Na^+/K^+$-ATPase α1 was found to be expressed in the apical membrane of post-natal mouse RPE (Figs. 2A'-2D', Table 1). In RPE of embryonic mice, however, $Na^+$-$K^+$/ATPase α1 was expressed on the basal side (Figs. 2Y and 2Z, Table 1), similar to findings in other types of epithelial cells (Amerongen et al., 1989; Sztul et al., 1987).

### *Ezrin*

Expression of ezrin, a marker for microvilli (Bonilha et al., 1999), was detected in the apical membranes of post-natal and mature mouse RPE (Figs. 2G'-2J', Table 1). In embryonic mouse RPE, however, ezrin expression was not polarized (Figs. 2E' and 2F', Table 1). These patterns were similar to those of F-actin, which is recruited by ezrin to the microvilli (Figs. 2K'-2P').

All of these results are summarized in Table 1 and low magnification images are provided in Supplementary Fig. S1.

## *Tsg101*-deficent embryonic RPE cells form random cell aggregates

Dynamic changes on the distribution of the adhesion and polarity markers in embryonic, post-natal, and mature RPE indicated that the localization of these proteins may be regulated by stage-specific environments, including changes in interactions of the RPE with the retina and ECM and in soluble factors produced by the RPE, retina, and choroid. These signals might not only induce the exocytic trafficking of proteins to the target sites, but may also induce their redistribution by endocytic down-regulation at unstable sites and/or their redistribution to stable sites (Rodriguez-Boulan and Macara, 2014; Shivas et al., 2010).

ESCRT complexes play important roles in the down-regulation of ubiquitinated proteins through the endo-lysosomal pathway (Luzio et al., 2009; Saksena et al., 2007). These complexes are also involved in the remobilization of membrane proteins via the fusion of MVBs to the plasma membrane. Furthermore, Tsg101, a component of ESCRT-I, was previously shown to establish the polarity of *Drosophila* embryonic cells (Moberg et al., 2005), suggesting that Tsg101 may also regulate developmental changes in RPE cell polarity in mice by remobilizing membrane proteins.

This hypothesis was tested by generating *$Tsg101^{fl/fl}$;TRP1-Cre* mice, in which the floxed *Tsg101* gene (*$Tsg101^{fl}$*) was deleted in *tyrosinase-related protein 1* (*TRP1*)-*Cre* affected RPE, ciliary epithelium, and cells in the peripheral retina (Mori et al., 2002; Wagner et al., 2003). Gross anatomical examination showed that eyes of *$Tsg101^{fl/fl}$;TRP1-Cre* mice, beginning at E14.5, were significantly smaller than in their *$Tsg101^{fl/+}$;TRP1-Cre* littermates (Fig. 3A, Supplementary Fig. S2). Moreover, RPE cells were depigmented in the eyes of *$Tsg101^{fl/fl}$;TRP1-Cre* mice (Fig. 3A). These depigmented RPE cells, however, still expressed microphthalmia factor 1 (Mitf1; Fig. 3B), a key transcription factor that induces the expression of melanin producing enzymes, such as *tyrosinase* and *TRP1* (Fang and Setaluri, 1999; Martinez-Morales et al., 2004). These results therefore suggest that depigmentation of the RPE may be associated with the involvement of Tsg101 in melanogenesis (Truschel et al., 2009), not with the trans-differentiation of RPE to other ocular cell types.

Mitf1-positive cells in *$Tsg101^{fl/fl}$;TRP1-Cre* mouse eyes, however, failed to form a monolayer epithelial sheet; rather, they formed irregular cell aggregates (Fig. 3B, Supplementary Fig. S2). These Mitf1-positive cells were positive for β-galactosidase (Fig. 3A), which was expressed from the *lacZ* Cre reporter knocked in the *ROSA26* gene locus (*R26R*) after the Cre-mediated deletion of the *loxP-STOP-loxP* gene cassette (Soriano, 1999), suggesting that impaired layer formation was an autonomous characteristic of *Tsg101*-deficient RPE. The numbers of Mitf1-positive cells were significantly lower in E14.5 *$Tsg101^{fl/fl}$;TRP1-Cre* mouse eyes than those in *$Tsg101^{fl/+}$;TRP1-Cre* littermate eyes (Figs. 3B and 3C). In contrast, the numbers of RPCs, which are positive for expression of visual system homeobox 2 (Vsx2) and SRY-Box transcription factor 2 (Sox2), and of post-mitotic retinal neurons, which are positive for expression of tubulinβ3 (Tuj1) and brain-specific homeobox 3b (Brn3b), did not differ markedly in the retinas of these mice (Supplementary Figs. S3A

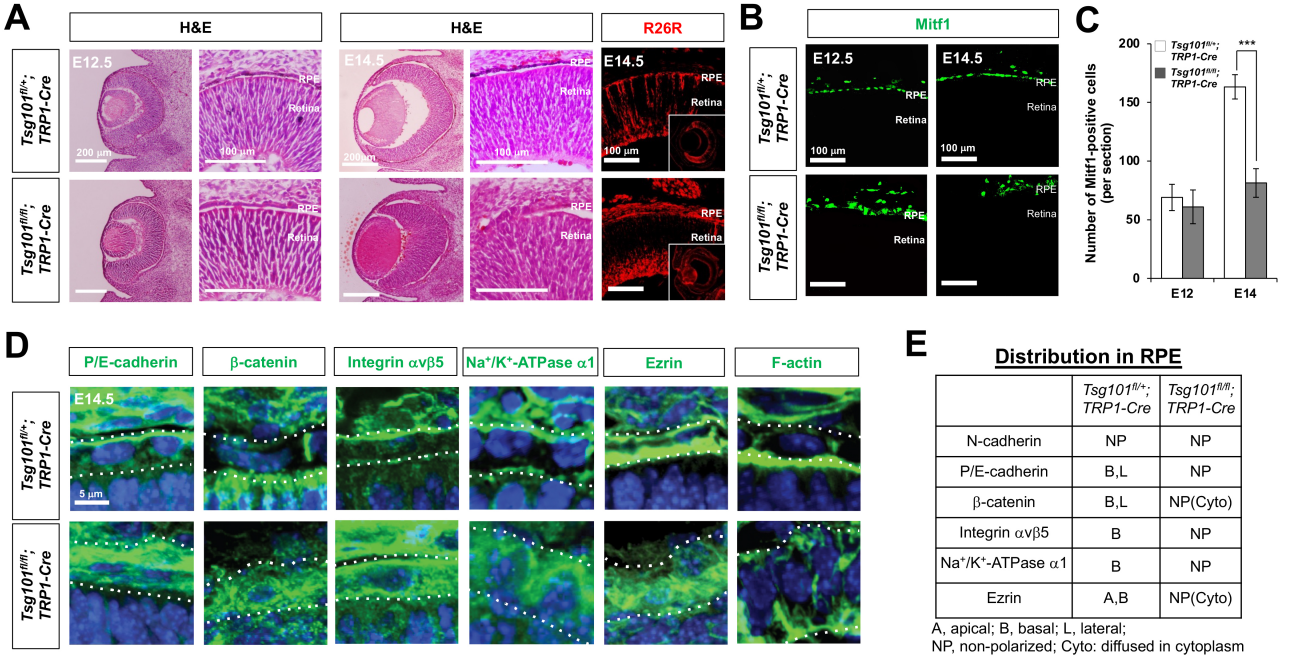


**Fig. 3. *Tsg101*-deficent embryonic RPE cells failed to form a monolayer structure.** (A) Morphologies of the embryonic mouse eyes were examined by H&E staining of eye sections of *Tsg101*$^{fl/+}$*;TRP1-Cre* and *Tsg101*$^{fl/fl}$*;TRP1-Cre* littermate mice at E12.5 and E14.5. The Cre-affected cells in E14.5 mouse eye sections was visualized by immunostaining of β-galactosidase expressed from *R26R* Cre reporter alleles. (B) Distribution of RPE in the littermate mouse eyes was examined by immunostaining of Mitf1. (C) The numbers of Mitf1-positive RPE in the mouse eyes were quantified and shown in the graph. Error bars denote SD (n = 4 from 4 independent litters). ***$P < 0.001$. (D and E) Distribution of polarity marker proteins in mouse RPE of E14.5 *Tsg101*$^{fl/+}$*;TRP1-Cre* and *Tsg101*$^{fl/fl}$*;TRP1-Cre* littermate mice was investigated by immunostaining (D) and the results are summarized in (E). Dash lines in (D) indicate basal (top) and apical (bottom) margins of RPE. Blue fluorescence signals are the nuclei stained by Hoe.

and S3B). The numbers of BrdU-labeled proliferative cells and pH3-positive mitotic cells at E14.5 also did not differ significantly in eyes of E14.5 *Tsg101*$^{fl/+}$*;TRP1-Cre* and *Tsg101*$^{fl/fl}$*;TRP1-Cre* mice (Supplementary Figs. S3C and S3D), suggesting that cell proliferation was not affected by the deletion of *Tsg101* from the RPE. The reduced numbers of RPE cells were not due to cell death, either, as there were no significant differences in the numbers of TUNEL-positive apoptotic cells in eyes of *Tsg101*$^{fl/fl}$*;TRP1-Cre* and *Tsg101*$^{fl/+}$*;TRP1-Cre* mice at E14.5 (Supplementary Figs. S3C and S3D). In contrast, the numbers of TUNEL-positive cells were significantly higher in E14.5 *Tsg101*$^{fl/fl}$*;Chx10-Cre* mouse eyes, in which *Tsg101* had been eliminated in RPCs and their descendent retinal neurons (Rowan and Cepko, 2004), than those in *Tsg101*$^{fl/+}$*;TRP1-Cre* littermate eyes (Supplementary Fig. S4). These results suggest that Tsg101 is essential for the survival of RPC and/or retinal neurons but not for the RPE, which requires it for monolayer formation and pigmentation.

## Deficiency of *Tsg101* in embryonic RPE leads to the loss of polarity

We next assessed whether the expression of the proteins, which exhibit the polarized distributions in embryonic RPE (Fig. 2, Table 1), was altered in *Tsg101*-deficient mouse embryonic RPE to form the cell aggregates. P/E-cadherin and β-catenin were detectable evenly in E14.5 *Tsg101*$^{fl/fl}$*;TRP1-Cre* mouse RPE, whereas those are accumulated in the apical and basal RPE of their *Tsg101*$^{fl/+}$*;TRP1-Cre* littermates (Figs. 3D [two left columns] and 3E). Integrin αvβ5, which was expressed on the basal side of RPE in *Tsg101*$^{fl/+}$*;TRP1-Cre* mice, was expressed evenly on both sides of the RPE in their *Tsg101*$^{fl/fl}$*;TRP1-Cre* littermates (Figs. 3D [third column from left] and 3E). $Na^+/K^+$-ATPase, a basal RPE marker of embryonic RPE (Fig. 2, Table 1), was found to be diffused throughout the entire RPE area of *Tsg101*$^{fl/fl}$*;TRP1-Cre* mice (Figs. 3D [third column from right] and 3E). Ezrin was also detected in the entire RPE cell area of *Tsg101*$^{fl/fl}$*;TRP1-Cre* mice, but it was enriched in the apical and basal RPE of *Tsg101*$^{fl/+}$*;TRP1-Cre* mice (Figs. 3D [second column from right] and 3E). Consequently, F-actin was failed to enrich in the apical side but diffused into the entire RPE area in *Tsg101*$^{fl/fl}$*;TRP1-Cre* mice (Fig. 3D, rightmost column). These results suggest that Tsg101 is necessary for the polarized distribution of these cell adhesion proteins in mouse embryonic RPE.

## *Tsg101*-deficient adult mouse RPE fails to form a monolayer sheet

Because the RPE aggregates could not be maintained in the eyes of *Tsg101*$^{fl/fl}$*;TRP1-Cre* embryos (Supplementary Fig. S2), we could not determine the polarity of mature RPE in these mice. We therefore bred *Tsg101*$^{fl/fl}$ mice with *Bestropin 1* (*BEST1*)*-Cre* mice to generate *Tsg101*$^{fl/fl}$*;BEST1-*

*Cre* mice, which lose *Tsg101* in the RPE at the adult stage (Iacovelli et al., 2011). Anatomical and histological analyses showed no significant differences in eyes between P60 *Tsg101*$^{fl/+}$*;BEST1-Cre* and *Tsg101*$^{fl/fl}$*;BEST1-Cre* mice, except for depigmentation of the eyes of the latter (Fig. 4A). However, the depigmented RPE cells in P60 *Tsg101*$^{fl/fl}$*;BEST1-Cre* mouse eyes failed to form a monolayer structure (Fig. 4B). Furthermore, the Otx2-positive RPE cells in the *Tsg101*$^{fl/fl}$*;BEST1-Cre* mouse eyes were present in higher numbers and stacked in multiple layers (Figs. 4B and 4C). However, the numbers of major retinal cell types, including Otx2-positive bipolar cells, in the eyes of *Tsg101*$^{fl/fl}$*;BEST1-Cre* and *Tsg101*$^{fl/+}$*;BEST1-Cre* mice did not differ significantly (Figs. 2B and 2C, Supplementary Fig. S5).

Analysis of the polarity of mouse RPE revealed that E-cadherin was expressed evenly on RPE membranes of *Tsg101*$^{fl/fl}$*;BEST1-Cre* mice, but was expressed strongly only at the AJs in *Tsg101*$^{fl/+}$*;BEST1-Cre* mice (Fig. 4D; leftmost column). Consequently, β-catenin was expressed throughout the entire RPE area in *Tsg101*$^{fl/fl}$*;BEST1-Cre* mice (Fig. 4D, second column from left). It was also shown that integrin αvβ5, $Na^+/K^+$-ATPase, and ezrin, which were detectable only in the apical regions of *Tsg101*$^{fl/+}$*;BEST1-Cre* mouse RPE, were expressed throughout the RPE in *Tsg101*$^{fl/fl}$*;BEST1-Cre* mice (Fig. 4D, three center columns). Similarly, F-actin, which was concentrated in the cell cortex of *Tsg101*$^{fl/+}$*;BEST1-Cre* mouse RPE, was expressed throughout the RPE in *Tsg101*$^{fl/fl}$*;BEST1-Cre* mice (Fig. 4D, rightmost column).

We further investigated ultrastructural alterations in the *Tsg101*-deficient mouse RPE by TEM. Intercellular adhesions of *Tsg101*$^{fl/fl}$*;BEST1-Cre* mouse RPE were disrupted and their basal folds became irregular (Fig. 4E, iii), findings likely due to the lack of basolateral enrichment of E-cadherin and β-catenin. However, microvilli were found to extend from the RPEs of both *Tsg101*$^{fl/+}$*;BEST1-Cre* and *Tsg101*$^{fl/fl}$*;BEST1-Cre* mice (arrows in Fig. 4E, ii and iv). However, the apical borders, from which the microvilli branched out, were detectable deeper in the *Tsg101*$^{fl/fl}$*;BEST1-Cre* mouse RPE (Fig. 4E, iv, blue dotted lines), suggesting that the apical-lateral borders do not form properly in the RPE of these mice, resulting in the growth of the microvilli even from the lateral sides.

## Activation of the EGFR signaling pathway in *Tsg101*-deficient RPE

Receptor tyrosine kinases (RTKs) are transported to the basolateral side of the RPEs, whereas their ligands are secreted from their apical side (Lehmann et al., 2014; Weisz and Rodriguez-Boulan, 2009). Consequently, the autocrine

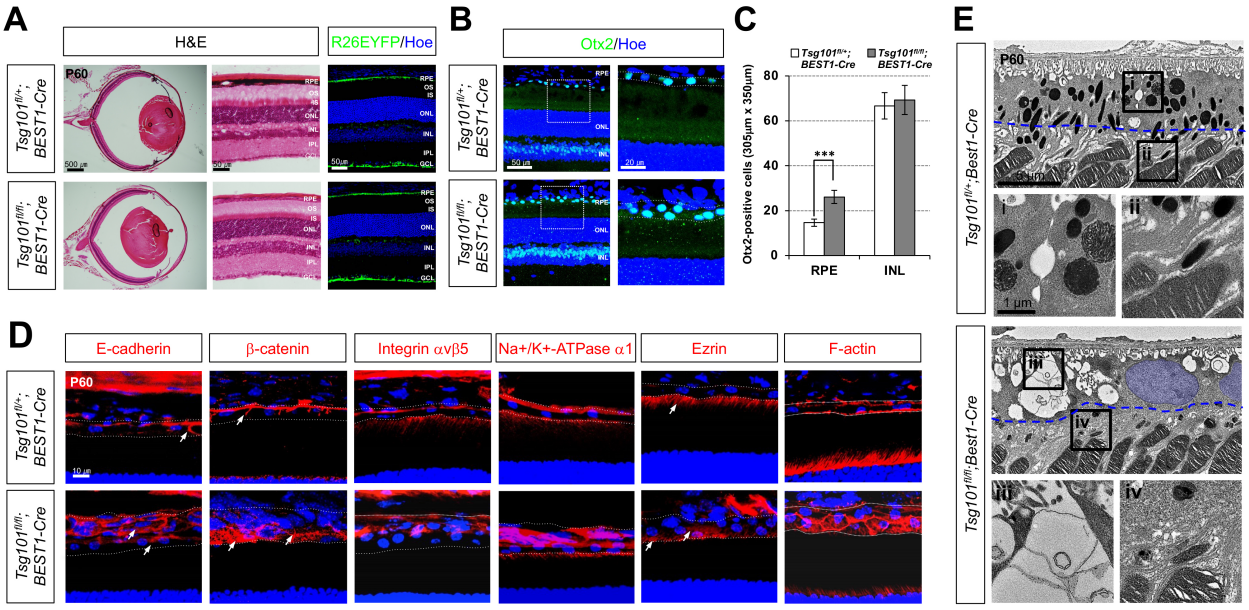


**Fig. 4. Deficiency of *Tsg101* in adult mouse RPE leads to the loss of polarity.** (A) Eye morphologies of *Tsg101*$^{fl/+}$*;BEST1-Cre* and *Tsg101*$^{fl/fl}$*;BEST1-Cre* littermate mice at P60 were examined by H&E staining of the eye sections. The Cre-affected cells in P60 mouse eye sections was visualized by immunostaining of EYFP expressed from *R26EYFP* Cre reporter alleles. OS, outer segments; IS, inner segments; ONL, outer nuclear layer; INL, inner nuclear layer; OPL, outer plexiform layer; IPL, inner plexiform layer; GCL, ganglion cell layer. (B) Distribution of Otx2-positive cells in the mouse eye sections was examined by immunostaining with anti-Otx2 antibody and nuclear counter staining with Hoe. The images in the right column are the magnified versions of the boxed RPE areas in the left column. (C) Numbers of Otx2-positive cells in RPE layer and the INL of the retinas were counted and shown in the graph. Error bars denote SD (n = 5 from 4 independent litters). ***$P < 0.001$. (D) Polarity of the mouse RPE was also investigated by immunostaining of the polarity markers. Dash lines indicate basal (top) and apical (bottom) margins of RPE. Blue fluorescence signals are nuclei stained by Hoe. (E) TEM images of RPE-retina interphase of P60 *Tsg101*$^{fl/+}$*;BEST1-Cre* and *Tsg101*$^{fl/fl}$*;BEST1-Cre* littermate mice. Two bottom images are the magnified versions of the boxed areas with corresponding numbers in top TEM images. RPE nuclear areas were pseudo-colored in blue. Blue dotted lines indicate the starting points of microvilli.

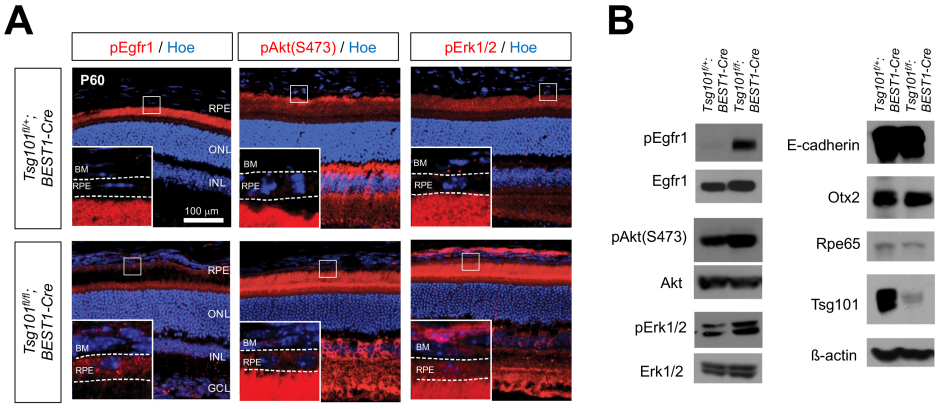


**Fig. 5. Activation of EGFR signaling in *Tsg101*-deficient RPE.** (A) Distribution of pEgfr1, pAkt, and pErk1/2 in P60 *Tsg101*$^{fl/+}$;*BEST1-Cre* and *Tsg101*$^{fl/fl}$;*BEST1-Cre* littermate mouse RPE was examined by immunostaining. Nuclei of RPE and retinal cells were stained by Hoe. The images in the insets are the magnified versions of the boxed areas in the same images. BM, Bruch's membrane; ONL, outer nuclear layer; INL, inner nuclear layer; GCL, ganglion cell layer. (B) Levels of indicated proteins in P60 mouse RPE was examined by western blot.

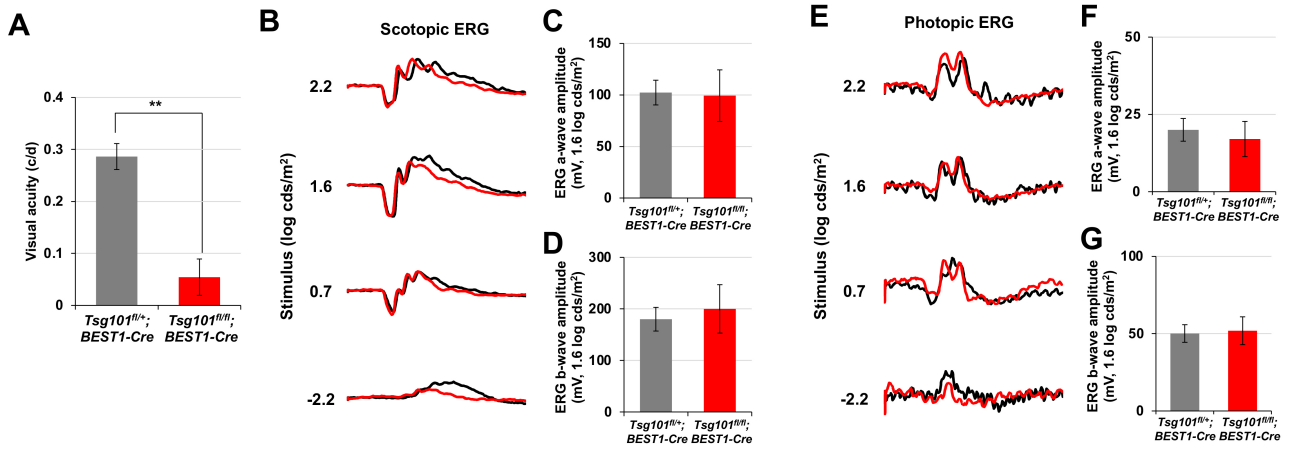


**Fig. 6. Normal retinal activity but impaired visual acuity of *Tsg101*$^{fl/fl}$;*BEST1-Cre* mice.** (A) Visual acuities of P60 *Tsg101*$^{fl/+}$;*BEST1-Cre* and *Tsg101*$^{fl/fl}$; *BEST1-Cre* littermate mice were measured by OptoMotry (see details in the Materials and Methods section). (B and E) Electrophysiological features of the retinas were investigated by electroretinogram (ERG) recordings of dark- or light-adapted mice. (C, D, F, and G) The amplitudes of ERG a- and b-waves of the mice were measured and the results are shown in the graphs. Error bars denote SD (n = 4, 4 independent litters).

activation of these RTKs, as represented by their phosphorylation, is suppressed in healthy epithelium. We found that the phosphorylation of epidermal growth factor receptor 1 (pEgfr1) was markedly increased in the RPE of *Tsg101*$^{fl/fl}$;*BEST1-Cre* mice, but was suppressed in the RPE of *Tsg101*$^{fl/+}$;*BEST1* mice (Fig. 5), suggesting the autocrine activation of Egfr1 in *Tsg101*-deficient RPE. This finding was supported by results showing that the activities of the downstream PI3K-Akt and MAPK pathways, which were shown to disrupt inter-RPE adhesion (Kang et al., 2009; Kim et al., 2008), were also elevated in the RPE of *Tsg101*$^{fl/fl}$;*BEST1-Cre* mice (Fig. 5). However, there was no evidence for the proliferation of RPE, which resumed the cell cycle and incorporated BrdU for one week (data not shown).

## Visual impairment of *Tsg101*$^{fl/fl}$;*BEST1-Cre* mice

The polarized RPE contributes to visual functions of the retina by maintaining the structures of photoreceptor outer segment and exchanging various materials with the photoreceptors (Simó et al., 2010; Strauss, 2005). We found that visual acuity was significantly impaired in P60 *Tsg101*$^{fl/+}$;*BEST1-Cre* mice (Fig. 6A), of which RPE had lost polarity but maintained contacts with the outer segments of photoreceptors (Fig. 4E). However, their electrophysiological activities, both the dark-adapted scotopic and light-adapted photopic responses measured by ERG, were normal (Figs. 6B-6G). The results suggest that the retinas adjacent to the depolarized *Tsg101*-deficient RPE could sense and process light but could not have spatial resolution. Collectively, our data suggest that

Tsg101 should be expressed in adult mouse RPE not only to maintaining RPE structures but also to supporting normal vision of the mice.

## DISCUSSION

The present study showed that cell adhesion proteins were differentially distributed in embryonic, perinatal, and mature RPE. The differences may be associated with differences in RPE functions during each state of development. RPE in embryos is not involved in vision as structural and functional supporters for the photoreceptors. The embryonic RPE does not develop the microvilli, which are projected from RPE apical membrane to interact with photoreceptor outer segments (Fig. 1). Instead, it forms junctional complexes with adjacent RPC to regulating retinal neurogenesis (Fig. 1) (Ha et al., 2017). Therefore, cadherins and β-catenin are not only expressed on the basolateral sides, but were also detected on the apical sides of the embryonic RPE, forming the junctional complexes with RPC. The transition from embryonic RPE-RPC interaction to mature RPE-photoreceptor interaction, which is less strong than embryonic RPE-RPC apical contacts, may therefore cause the redistribution of cadherins and β-catenin to the lateral side, where they form AJs (Fig. 2, Table 1). The transition on RPE-retinal interaction also moves ezrin exclusively on the apical sides to support the extension of microvilli (Fig. 2, Table 1). Integrin αvβ5 is also localized at the apical side due to its function in the phagocytosis of photoreceptor outer segments (Finnemann et al., 1997). $Na^+$-$K^+$/ATPase-α1 was also found to localize to the apical surface of mature RPE. On the contrary, $Na^+$-$K^+$/ATPase-α1 is enriched on the baso-lateral sides of embryonic RPE as it is in other epithelial cell types (Marmorstein, 2001; Shimura et al., 1999). This difference may be associated with the function of $Na^+$-$K^+$/ATPase-α1 in phototransduction. $Na^+$-$K^+$/ATPase-α1 on the apical side of the RPE exports $Na^+$ ions into the subretinal space for the depolarization of unstimulated photoreceptors (Gallemore et al., 1997). These apical markers were still observed in the apical membrane of *Tsg101*-deficient mouse RPE, whereas E-cadherin and β-catenin cannot be maintained in the baso-lateral sides (Fig. 4D). Consequently, *Tsg101*-deficient mouse RPE maintains microvilli (Fig. 4E) and ERG responses (Figs. 6B-6G). The results suggest that Tsg101-dependent protein downregulation and/or redistribution are more critical for the proteins on the basolateral than on the apical side of the RPE.

ESCRT components in *Drosophila* were reported to have tumor suppressor properties (Herz et al., 2006; Moberg et al., 2005; Vaccari and Bilder, 2005). Notch activity in *dTsg101*-deficient cells was elevated, leading to the proliferation of neighboring cells through activation of the JAK-STAT pathway (Moberg et al., 2005). Unlike *dTsg101*, mouse *Tsg101* did not show tumor suppressor activity, but was necessary for cell survival (Wagner et al., 2003). The anti-apoptotic characteristics of mouse *Tsg101* were also seen in *Tsg101*-deficient retinas, which lost cells by massive apoptosis (Supplementary Fig. S4). However, *Tsg101* in mouse RPE showed neither tumor suppressor nor cell survival factor activity (Figs. 3 and 4, Supplementary Figs. S3C and S3D). Moreover, unlike *dTsg101*-deficient cells (Moberg et al., 2005), loss of *Tsg101* did not increase Notch receptor levels in the RPE (data not shown). In contrast, the level of pEGFR, which accumulates in endocytic vesicles upon activation (Adamson and Rees, 1981; Bakker et al., 2017), was increased in *Tsg101*-deficient mouse RPE, activating the downstream anti-apoptotic PI3K-Akt and MAPK signaling pathways (Fig. 5). Consequently, it might suppress the death of the cells. Despite the activation of the EGFR-PI3K-Akt signaling pathway, which enhances cell proliferation, RPE did not proliferate actively but lost the polarized epithelial characteristics. This is reminiscent to *Pten*-deficient RPE, which was depolarized and exhibited hyperactive Akt but did not proliferate in adult mice (Kim et al., 2008). These results suggest that the distributions of RTKs and their ligands should be regulated tightly in RPE to prevent the overactivation of PI3K-Akt pathway.

Despite the loss of cell polarity, retinal structures, as determined by retinal cell composition, and functions, as measured by ERG, appeared normal in *Tsg101$^{fl/fl}$;BEST1-Cre* mouse retinas (Figs. 6B-6G, Supplementary Fig. S5). However, their spatial resolutions were significantly compromised (Fig. 6A). The marked reduction in light-absorbing melanin granules in the RPE of *Tsg101$^{fl/fl}$;BEST1-Cre* mice may impair the absorption of scattered light from the photoreceptors. Consequently, the spatial differences between the photoreceptors might interfere with the scattered light, resulting in the reduced visual acuity of the mice.

*Note: Supplementary information is available on the Molecules and Cells website (www.molcells.org).*

## ACKNOWLEDGMENTS

This work was supported by the National Research Foundation of Korea (NRF) grants (NRF-2017R1A2B3002862 and NRF-2018R1A5A1024261) funded by Korean Ministry of Science and ICT (MSIT), South Korea.

We appreciate for Drs. Mark, Dunaief, and Cepko for the generous gifts for *TRP1-Cre*, *BEST1-Cre*, and *Chx10-Cre* mice. We appreciate for technical services of KAIST Laboratory Resource Center and BioCore Center.

## AUTHOR CONTRIBUTIONS

D.L. and S.L. conceived and performed experiments, and wrote the manuscript. K.W.M., J.W.P., Y.K., T.H., and K.H.M. performed experiments. K.U.W. provided the Tsc1-flox mice. J.W.K. conceived and supervised the experiments, wrote the manuscript, and secured funding.

## CONFLICT OF INTEREST

The authors have no potential conflicts of interest to disclose.

## ORCID

| | |
|---|---|
| Dai Le | https://orcid.org/0000-0001-6395-6163 |
| Soyeon Lim | https://orcid.org/0000-0003-3106-2282 |
| Kwang Wook Min | https://orcid.org/0000-0002-7593-7047 |
| Joon Woo Park | https://orcid.org/0000-0003-2467-5750 |
| Youjoung Kim | https://orcid.org/0000-0003-4089-8292 |
| Taejeong Ha | https://orcid.org/0000-0003-1664-1593 |
| Kyeong Hwan Moon | https://orcid.org/0000-0001-9868-2238 |

Kay-Uwe Wagner https://orcid.org/0000-0002-5081-0226
Jin Woo Kim https://orcid.org/0000-0003-0767-1918

## REFERENCES

Adamson, E.D. and Rees, A.R. (1981). Epidermal growth factor receptors. Mol. Cell. Biochem. *34*, 129-152.

Amerongen, H.M., Mack, J.A., Wilson, J.M., and Neutra, M.R. (1989). Membrane domains of intestinal epithelial cells: distribution of $Na^+$,$K^+$-ATPase and the membrane skeleton in adult rat intestine during fetal development and after epithelial isolation. J. Cell Biol. *109*, 2129-2138.

Babst, M. (2011). MVB vesicle formation: ESCRT-dependent, ESCRT-independent and everything in between. Curr. Opin. Cell Biol. *23*, 452-457.

Bakker, J., Spits, M., Neefjes, J., and Berlin, I. (2017). The EGFR odyssey - from activation to destruction in space and time. J. Cell Sci. *130*, 4087-4096.

Bonilha, V.L., Finnemann, S.C., and Rodriguez-Boulan, E. (1999). Ezrin promotes morphogenesis of apical microvilli and basal infoldings in retinal pigment epithelium. J. Cell Biol. *147*, 1533-1548.

Burke, J.M., Cao, F., Irving, P.E., and Skumatz, C.M.B. (1999). Expression of E-cadherin by human retinal pigment epithelium: delayed expression in vitro. Invest. Ophthalmol. Vis. Sci. *40*, 2963-2970.

Burke, J.M. and Hong, J. (2006). Fate of E-cadherin in early RPE cultures: transient accumulation of truncated peptides at nonjunctional sites. Invest. Ophthalmol. Vis. Sci. *47*, 3635-3643.

Cachafeiro, M., Bemelmans, A.P., Samardzija, M., Afanasieva, T., Pournaras, J.A., Grimm, C., Kostic, C., Philippe, S., Wenzel, A., and Arsenijevic, Y. (2013). Hyperactivation of retina by light in mice leads to photoreceptor cell death mediated by VEGF and retinal pigment epithelium permeability. Cell Death Dis. *4*, e781.

Clague, M.J., Liu, H., and Urbe, S. (2012). Governance of endocytic trafficking and signaling by reversible ubiquitylation. Dev. Cell *23*, 457-467.

Eden, E.R., White, I.J., and Futter, C.E. (2009). Down-regulation of epidermal growth factor receptor signalling within multivesicular bodies. Biochem. Soc. Trans. *37*, 173-177.

Fang, D. and Setaluri, V. (1999). Role of microphthalmia transcription factor in regulation of melanocyte differentiation marker TRP-1. Biochem. Biophys. Res. Commun. *256*, 657-663.

Finnemann, S.C., Bonilha, V.L., Marmorstein, A.D., and Rodriguez-Boulan, E. (1997). Phagocytosis of rod outer segments by retinal pigment epithelial cells requires alpha(v)beta5 integrin for binding but not for internalization. Proc. Natl. Acad. Sci. U. S. A. *94*, 12932-12937.

Fujimura, N., Taketo, M.M., Mori, M., Korinek, V., and Kozmik, Z. (2009). Spatial and temporal regulation of Wnt/β-catenin signaling is essential for development of the retinal pigment epithelium. Dev. Biol. *334*, 31-45.

Gallemore, R.P., Hughes, B.A., and Miller, S.S. (1997). Retinal pigment epithelial transport mechanisms and their contributions to the electroretinogram. Prog. Retin. Eye Res. *16*, 509-566.

Grant, B.D. and Donaldson, J.G. (2009). Pathways and mechanisms of endocytic recycling. Nat. Rev. Mol. Cell Biol. *10*, 597-608.

Gruenberg, J. and Stenmark, H. (2004). The biogenesis of multivesicular endosomes. Nat. Rev. Mol. Cell Biol. *5*, 317-323.

Gundersen, D., Orlowski, J., and Rodriguez-Boulan, E. (1991). Apical polarity of Na,K-ATPase in retinal pigment epithelium is linked to a reversal of the ankyrin-fodrin submembrane cytoskeleton. J. Cell Biol. *112*, 863-872.

Ha, T., Moon, K.H., Dai, L., Hatakeyama, J., Yoon, K., Park, H.S., Kong, Y.Y., Shimamura, K., and Kim, J.W. (2017). The retinal pigment epithelium is a Notch signaling niche in the mouse retina. Cell Rep. *19*, 351-363.

Herz, H.M., Chen, Z., Scherr, H., Lackey, M., Bolduc, C., and Bergmann, A. (2006). vps25 mosaics display non-autonomous cell survival and overgrowth, and autonomous apoptosis. Development *133*, 1871-1880.

Hurley, J.H. (2010). The ESCRT complexes. Crit. Rev. Biochem. Mol. Biol. *45*, 463-487.

Iacovelli, J., Zhao, C., Wolkow, N., Veldman, P., Gollomp, K., Ojha, P., Lukinova, N., King, A., Feiner, L., Esumi, N., et al. (2011). Generation of Cre transgenic mice with postnatal RPE-specific ocular expression. Invest. Ophthalmol. Vis. Sci. *52*, 1378-1383.

Imamura, Y., Noda, S., Hashizume, K., Shinoda, K., Yamaguchi, M., Uchiyama, S., Shimizu, T., Mizushima, Y., Shirasawa, T., and Tsubota, K. (2006). Drusen, choroidal neovascularization, and retinal pigment epithelium dysfunction in SOD1-deficient mice: a model of age-related macular degeneration. Proc. Natl. Acad. Sci. U. S. A. *103*, 11282-11287.

Kang, K.H., Lemke, G., and Kim, J.W. (2009). The PI3K-PTEN tug-of-war, oxidative stress and retinal degeneration. Trends Mol. Med. *15*, 191-198.

Kim, J.W., Kang, K.H., Burrola, P., Mak, T.W., and Lemke, G. (2008). Retinal degeneration triggered by inactivation of PTEN in the retinal pigment epithelium. Genes Dev. *22*, 3147-3157.

Kim, Y., Lim, S., Ha, T., Song, Y.H., Sohn, Y.I., Park, D.J., Paik, S.S., Kim-Kaneyama, J.R., Song, M.R., Leung, A., et al. (2017). The LIM protein complex establishes a retinal circuitry of visual adaptation by regulating Pax6 alpha-enhancer activity. Elife *6*, e21303.

Le Borgne, R. and Hoflack, B. (1998). Protein transport from the secretory to the endocytic pathway in mammalian cells. Biochim. Biophys. Acta *1404*, 195-209.

Lehmann, G.L., Benedicto, I., Philp, N.J., and Rodriguez-Boulan, E. (2014). Plasma membrane protein polarity and trafficking in RPE cells: past, present and future. Exp. Eye Res. *126*, 5-15.

Luzio, J.P., Piper, S.C., Bowers, K., Parkinson, M.D.J., Lehner, P.J., and Bright, N.A. (2009). ESCRT proteins and the regulation of endocytic delivery to lysosomes. Biochem. Soc. Trans. *37*(Pt 1), 178-180.

Marmorstein, A.D. (2001). The polarity of the retinal pigment epithelium. Traffic *2*, 867-872.

Martinez-Morales, J.R., Rodrigo, I., and Bovolenta, P. (2004). Eye development: a view from the retina pigmented epithelium. Bioessays *26*, 766-777.

Mellman, I. and Nelson, W.J. (2008). Coordinated protein sorting, targeting and distribution in polarized cells. Nat. Rev. Mol. Cell Biol. *9*, 833-845.

Moberg, K.H., Schelble, S., Burdick, S.K., and Hariharan, I.K. (2005). Mutations in erupted, the Drosophila ortholog of mammalian tumor susceptibility gene 101, elicit non-cell-autonomous overgrowth. Dev. Cell *9*, 699-710.

Mori, M., Gargowitsch, L., Bornert, J.M., Garnier, J.M., Mark, M., Chambon, P., and Metzger, D. (2012). Temporally controlled targeted somatic mutagenesis in mouse eye pigment epithelium. Genesis *50*, 828-832.

Mori, M., Metzger, D., Garnier, J.M., Chambon, P., and Mark, M. (2002). Site-specific somatic mutagenesis in the retinal pigment epithelium. Invest. Ophthalmol. Vis. Sci. *43*, 1384-1388.

Morita, E. (2012). Differential requirements of mammalian ESCRTs in multivesicular body formation, virus budding and cell division. FEBS J. *279*, 1399-1406.

Prusky, G.T., Alam, N.M., Beekman, S., and Douglas, R.M. (2004). Rapid quantification of adult and developing mouse spatial vision using a virtual optomotor system. Invest. Ophthalmol. Vis. Sci. *45*, 4611-4616.

Rodriguez-Boulan, E. and Macara, I.G. (2014). Organization and execution of the epithelial polarity programme. Nat. Rev. Mol. Cell Biol. *15*, 225-242.

Rowan, S. and Cepko, C.L. (2004). Genetic analysis of the homeodomain transcription factor Chx10 in the retina using a novel multifunctional BAC transgenic mouse reporter. Dev. Biol. *271*, 388-402.

Saksena, S., Sun, J., Chu, T., and Emr, S.D. (2007). ESCRTing proteins in the endocytic pathway. Trends Biochem. Sci. *32*, 561-573.

Schmidt, O. and Teis, D. (2012). The ESCRT machinery. Curr. Biol. *22*, R116-R120.

Shimura, M., Kakazu, Y., Oshima, Y., Tamai, M., and Akaike, N. (1999). Na+,K+-ATPase activity in cultured bovine retinal pigment epithelium. Invest. Ophthalmol. Vis. Sci. *40*, 96-104.

Shivas, J.M., Morrison, H.A., Bilder, D., and Skop, A.R. (2010). Polarity and endocytosis: reciprocal regulation. Trends Cell Biol. *20*, 445-452.

Simó, R., Villarroel, M., Corraliza, L., Hernández, C., and Garcia-Ramírez, M. (2010). The retinal pigment epithelium: something more than a constituent of the blood-retinal barrier - implications for the pathogenesis of diabetic retinopathy. J. Biomed. Biotechnol. *2010*, 190724.

Soriano, P. (1999). Generalized lacZ expression with the ROSA26 Cre reporter strain. Nat. Genet. *21*, 70-71.

Strauss, O. (2005). The retinal pigment epithelium in visual function. Physiol. Rev. *85*, 845-881.

Sztul, E.S., Biemesderfer, D., Caplan, M.J., Kashgarian, M., and Boyer, J.L. (1987). Localization of Na+,K+-ATPase alpha-subunit to the sinusoidal and lateral but not canalicular membranes of rat hepatocytes. J. Cell Biol. *104*, 1239-1248.

Truschel, S.T., Simoes, S., Gangi Setty, S.R., Harper, D.C., Tenza, D., Thomas, P.C., Herman, K.E., Sackett, S.D., Cowan, D.C., Theos, A.C., et al. (2009). ESCRT-I function is required for Tyrp1 transport from early endosomes to the melanosome limiting membrane. Traffic *10*, 1318-1336.

Vaccari, T. and Bilder, D. (2005). The Drosophila tumor suppressor vps25 prevents nonautonomous overproliferation by regulating notch trafficking. Dev. Cell *9*, 687-698.

Veleri, S., Lazar, C.H., Chang, B., Sieving, P.A., Banin, E., and Swaroop, A. (2015). Biology and therapy of inherited retinal degenerative disease: insights from mouse models. Dis. Model. Mech. *8*, 109-129.

Wagner, K.U., Krempler, A., Qi, Y., Park, K., Henry, M.D., Triplett, A.A., Riedlinger, G., Rucker III, E.B., and Hennighausen, L. (2003). Tsg101 is essential for cell growth, proliferation, and cell survival of embryonic and adult tissues. Mol. Cell. Biol. *23*, 150-162.

Weisz, O.A. and Rodriguez-Boulan, E. (2009). Apical trafficking in epithelial cells: signals, clusters and motors. J. Cell Sci. *122*, 4253-4266.

Williams, S.K., Greener, D.A., and Solenski, N.J. (1984). Endocytosis and exocytosis of protein in capillary endothelium. J. Cell. Physiol. *120*, 157-162.

Xu, L., Overbeek, P.A., and Reneker, L.W. (2002). Systematic analysis of E-, N- and P-cadherin expression in mouse eye development. Exp. Eye Res. *74*, 753-760.